Title	Dead space effect in space-charge region of collector of AlGaAs/InGaAs p-n-p heterojunction bipolar transistors
Author(s)	Yan, BP; Wang, XQ; Yang, ES
Citation	Journal Of Applied Physics, 2001, v. 90 n. 10, p. 5351-5356
Issued Date	2001
URL	http://hdl.handle.net/10722/42114
Rights	Journal of Applied Physics. Copyright © American Institute of Physics.

Dead space effect in space-charge region of collector of AlGaAs/InGaAs *p-n-p* heterojunction bipolar transistors

B. P. Yan,[a] X. Q. Wang, and E. S. Yang
Department of Electrical and Electronic Engineering, The University of Hong Kong, Pokfulam Road, Hong Kong

(Received 17 January 2001; accepted for publication 17 August 2001)

Hole-initiated avalanche multiplication is investigated using an AlGaAs/InGaAs *p-n-p* heterojunction bipolar transistor (HBT). Both experimental measurements and theoretical calculation are used to determine the avalanche multiplication factor. A large departure is observed at low electric field when comparison is made between the measured data and theoretical results obtained from the standard ionization model. The comparison shows that the conventional impact ionization model, based on local electric field, substantially overestimates the hole avalanche multiplication factor $M_p - 1$ in the AlGaAs/InGaAs *p-n-p* HBT, where a significant dead space effect occurs in the collector space-charge region. A simple correction model for the dead space is proposed, that allows the multiplication to be accurately predicted, even in a heavily doped structure. Based on this model, multiplication characteristics for different threshold energy of the hole are calculated. A threshold energy of 2.5 eV was determined to be suitable for describing the hole-initiated impact ionization process. © *2001 American Institute of Physics.*
[DOI: 10.1063/1.1412836]

I. INTRODUCTION

Heterojunction bipolar transistors (HBTs) based on III–V compound semiconductors have shown great potential both for high-speed circuits and for microwave power application.[1,2] For the operation of a power HBT, avalanche multiplication connected to impact ionization is of fundamental importance, because it determines the breakdown voltage. Electron avalanche multiplication in AlGaAs/GaAs,[3–6] InGaP/GaAs,[7] and InP/GaInAs (Ref. 8) *n-p-n* HBTs has been intensively investigated. By contrast, no effort was devoted to hole-initiated avalanche multiplication and ionization coefficient, even though the *p-n-p* HBT has recently attracted much attention because of their applications in monolithic complementary HBT technology.[9,10] Since calculation of the breakdown voltage needs both carrier multiplication factors, understanding of the hole avalanche multiplication and ionization coefficient in the *p-n-p* HBT is necessary. In this article, the hole-initiated avalanche multiplication is investigated using a specially designed AlGaAs/InGaAs *p-n-p* HBT. Both experimental measurements and theoretical calculation are used to determine the hole-initiated avalanche multiplication factor. Our results show that there is also a strong dead space effect in the space-charge region of the collector of AlGaAs/InGaAs *p-n-p* HBTs and the conventional impact ionization model based on local electric field largely overestimates the avalanche multiplication in AlGaAs/InGaAs *p-n-p* HBTs. A simple correction model is proposed, which is found to provide a good agreement with experimental results when threshold energy of 2.5 eV is assumed to describe the hole-initiated impact ionization processes.

II. DEVICE FABRICATION AND PERFORMANCE

In order to investigate the hole-initiated avalanche multiplication phenomena, a specially designed AlGaAs/InGaAs *n-p-n* HBT structure was grown on a semi-insulating GaAs substrate by molecular beam epitaxy. In view of the low hole mobility in GaAs, an indium composition in the InGaAs base was linearly graded from 15% at the collector edge to 0% at the emitter edge to reduce the base transit time. The device structure consists of a 700 nm $p=3\times10^{19}\,\mathrm{cm}^{-3}$ GaAs subcollector, a 250 nm $p=5\times10^{16}\,\mathrm{cm}^{-3}$ GaAs collector, a 15 nm $p=5\times10^{16}\,\mathrm{cm}^{-3}$ $In_xGa_{1-x}As$ graded layer ($x=0-0.15$), a 10 nm $p=5\times10^{16}\,\mathrm{cm}^{-3}$ $In_{0.15}Ga_{0.85}As$ spacer layer, a 50 nm $n=5\times10^{18}\,\mathrm{cm}^{-3}$ $In_xGa_{1-x}As$ compositionally graded base ($x=0.15-0$), a 70 nm $p=5\times10^{17}\,\mathrm{cm}^{-3}$ AlGaAs emitter with graded layers at two sides, a 80 nm $p=1\times10^{18}\,\mathrm{cm}^{-3}$ GaAs cap layer, and a 20 nm $p=5\times10^{19}\,\mathrm{cm}^{-3}$ GaAs ohmic contact layer.

Device fabrication began with an evaporating emitter electrode (Ti/Pt/Au). An emitter mesa was subsequently defined and the regions other than the emitter mesas were wet etched down to the base surface. It should be noted that, because the base layer thickness of the AlGaAs/InGaAs *p-n-p* HBT is much thinner than that of common AlGaAs/GaAs *p-n-p* HBT, it is necessary to use the selective etching solution to prevent etching past the base layer. In this study, two etching solutions are employed. The first solution is 10:4:500 $NH_4OH:H_2O_2:H_2O$ solution, and it is used to etch down to approximately 500 Å above the n^+ InGaAs base layer. The second etching solution is the

[a]Author to whom correspondence should be addressed; electronic mail: bpyan@eee.hku.hk

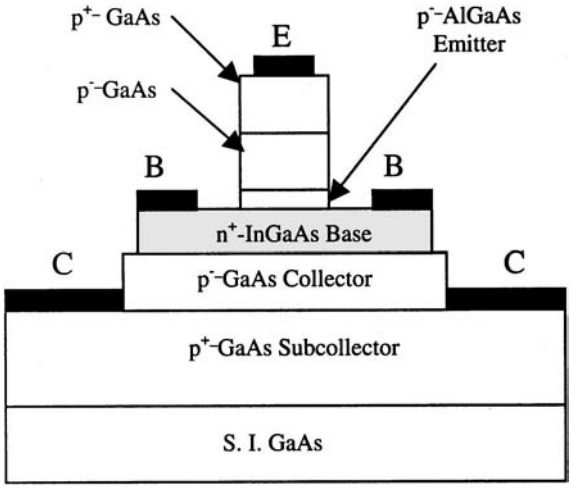

FIG. 1. The cross section of fabricated HBT structure.

$K_3Fe(CN)_6/K_4Fe(CN)_6$ selective solution. This so-called ''ferric-ferro cyanide solution'' can selectively etch AlGaAs but stop at InGaAs when its *p*H value is adjusted to 7.[9] The selectivity is very high, and no situations of etching past the base layer had occurred. Next, the base contact region was defined and a base contact metal of Pd/Ge/Ti/Au was deposited by *e*-beam evaporation. It should be noted that Pd/Ge/Ti/Au was used as the base contact, while the common *n*-type alloyed ohmic contact system Au/Ge/Ni/Au is not used. This is because the base thickness for a typical rf *p-n-p* HBT is between 30 and 50 nm. Alloying of the above metal contact causes the metal to spike through the base layer, leading to a short through the base–collector junction. After forming the base contact, the collector was defined and contact metal of Ti/Au was used. The contact was alloyed at 400 °C for 10 s to form ohmic contact. Figure 1 shows the cross section of the fabricated HBT structure.

dc characterization was made with a HP 4155 parameter analyzer. Measured devices have an emitter area of $35\,\mu m \times 45\,\mu m$. Typical common-emitter current–voltage ($I-V$) characteristics are shown in Fig. 2. It can be seen that the emitter–collector offset voltage is 350 mV. The emitter–collector breakdown voltage, BV_{CE0}, is measured as 6.8 V.

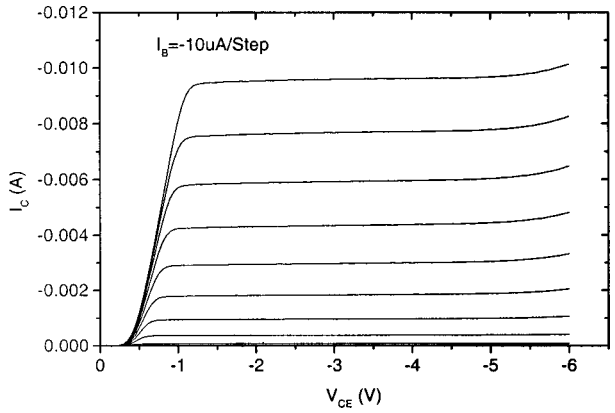

FIG. 2. Common emitter current–voltage ($I-V$) characteristics of the *p-n-p* AlGaAs/InGaAs HBT.

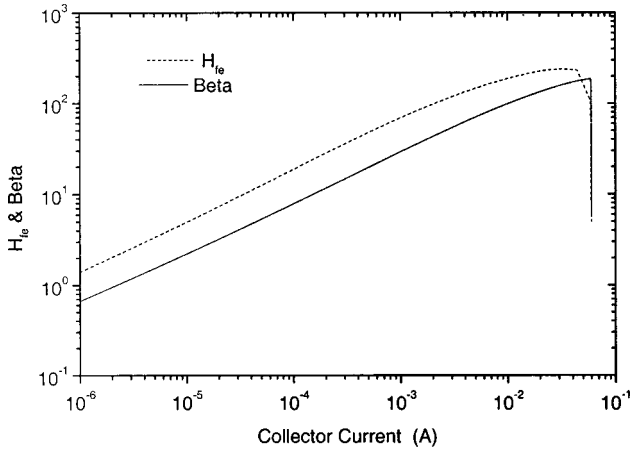

FIG. 3. Measured dc beta and H_{fe} as a function of collector current.

This BV_{CE0} value is expected for these measured HBTs whose collector is only 250 nm, even though the base–collector junction contains a portion of the narrow band gap InGaAs material. dc current gain β and incremental current gain H_{fe} as functions of collector current are shown in Fig. 3. As shown the current gain continues to increase with collector current, and reaches a maximum value of 186 before it suddenly decreases. The observation that the current gain never saturates at a constant value indicates that the base–emitter space charge region recombination current, rather than the base bulk recombination current, is a main base current component. In a large area device, both the extrinsic base surface recombination current and the base contact recombination current can be negligible compared to the base bulk recombination current, because the former two components are proportional to the emitter periphery, whereas the latter is proportional to the device area.[11] The electron back-injection current is also negligible together at room temperature. Therefore, the two important components are the base bulk recombination current and the space-charge recombination current. For our device, base doping is only moderate, so the dominant base current should be the space-charge recombination current, not the bulk recombination current. This is confirmed by the Gummel plots shown in Fig. 4. As shown

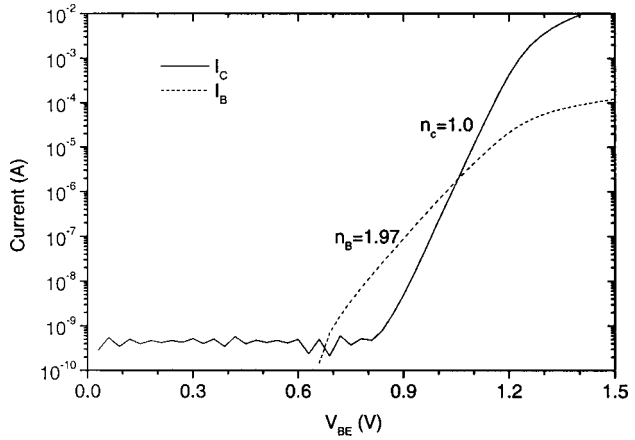

FIG. 4. Measured Gummel plot of the *p-n-p* AlGaAs/InGaAs HBT.

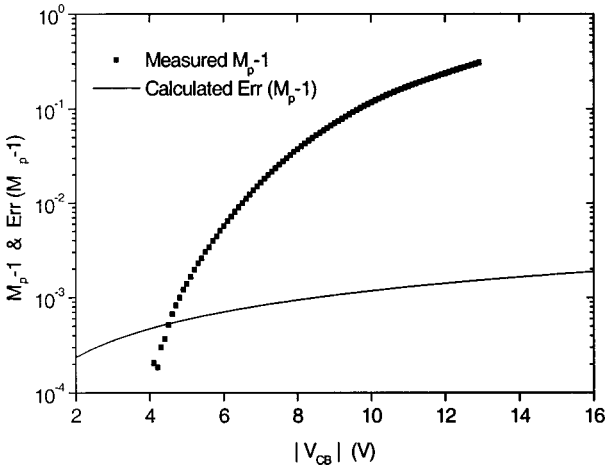

FIG. 5. M_p-1 and Err(M_p-1) as a function of the collector–base voltage $|V_{CB}|$.

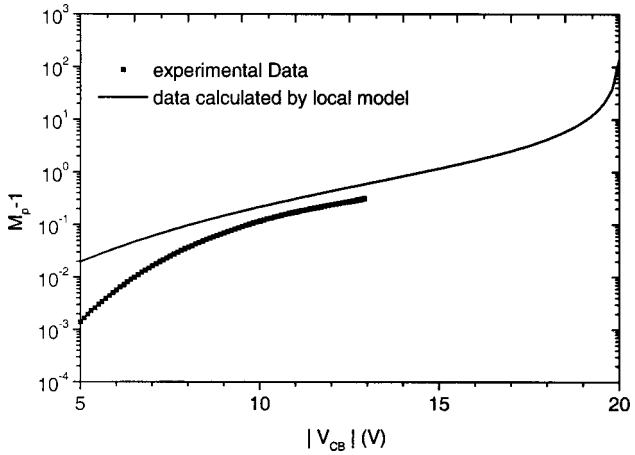

FIG. 6. Measured multiplication factor as a function of applied voltage in AlGaAs/InGaAs *p-n-p* HBT. Solid line shows data calculated using the local model and dots show measured data.

in Fig. 4, the measured I_B ideality factor is 1.97, very close to the factor of 2, which is the ideality factor of the space-charge recombination current. The large space charge recombination current most likely results from the fact that the depletion region adjacent to the base layer, in which most recombination events take place, is made of narrow GaAs. Thus, the larger thermal carrier concentration associated with narrow band gap material leads to a higher recombination current than expected from abrupt HBTs. In contrast, the base bulk recombination current is small because both a base quasielectric field and a moderate base doping are used.

III. AVALANCHE MULTIPLICATION CHARACTERISTICS

A. Measurement method

To obtain the multiplication characteristics as a function of the electric field, the technique described by Zanoni[3] and Canali *et al.*[5] was used. The HBT was operated in the common base mode and a constant base-emitter bias $V_{BE}=1.15\,\mathrm{V}$ was applied to inject the hole into the base to be collected by a collector. Generated electrons are collected at the base contact, which contribute to a negative term ΔI_B in the base current:[3,5]

$$\Delta I_B = I_B(V_{CB}) - I_{B0}, \tag{1}$$

where I_{B0} is the base current without multiplication and it is assumed to be equal to I_B at $V_{CB}=0\,\mathrm{V}$. Under conditions when the multiplication value is high, the base current may reverse its polarity and become negative. The multiplication factor M_p-1 can be evaluated from[3,5]

$$M_p - 1 = \frac{|\Delta I_B|}{I_C - |\Delta I_B|}, \tag{2}$$

B. Consideration of parasitic effects

There are three parasitic effects which influence the measurement of an avalanche multiplication factor. They are the base–collector junction reverse current I_{CB0}, the Early effect, and the self-heating effect of the device, respectively. The base–collector diode reverse current I_{CB0} measured at $I_E=0$ was very low (10 pA at $V_{CB}=13\,\mathrm{V}$) thus the parasitic contribution of I_{CB0} can be neglected. Since the current is not very high, the self-heating of the device can also be neglected in our measurement. The Early effect is significant at the condition of low bias but can be neglected at the condition of high bias. In order to verify that the Early effect does not contribute significantly to the results, the error introduced by the Early effect, Err (M_p-1), has been calculated according to the method proposed by Shamir and Ritter.[12] Figure 5 shows the measured avalanche multiplication factor M_p-1 and the error introduced by the Early effect, Err (M_p-1). It can be seen from Fig. 5 that Err (M_p-1) is much smaller than M_p-1 under the condition of $V_{CB} \geqslant 5\,\mathrm{V}$. Therefore, the contribution of the Early effect to M_p-1 is negligible under the condition of measurement.

C. Measurement results and theoretical analysis

Figure 6 shows the theoretical and experimental multiplication factor M_p-1 as a function of applied voltage. The solid line shows the calculated theoretical values of M_p-1 using the traditional local electric field model, which is given by the expression[13]

$$M_p - 1 = \frac{1}{1 - \int_0^{W_C} \alpha_p(x) \exp\{-\int_0^x [\alpha_p(x') - \alpha_n(x')]dx'\}dx} - 1, \tag{3}$$

where $\alpha_p(x)$ and $\alpha_n(x)$ are the hole and electron ionization coefficients, respectively, as a function of distance, and W_C is the width of collector space-charge region. The field dependence of the electron and hole ionization coefficient α_n and α_p is given, according to Bulman *et al.*,[14] respectively, by the expressions

$$\alpha_n(E(x)) = 1.899\times 10^5 \exp\{-[5.570\times 10^5/E(x)]^{1.82}\}, \tag{4}$$

$$\alpha_p(E(x)) = 2.215\times 10^5 \exp\{-[6.570\times 10^5/E(x)]^{1.75}\}, \quad (5)$$

where $E(x)$ is the electric field profile in the space-charge region of the collector with the maximum electric field occurring at $x=0$. It should be pointed out that α_n and α_p were determined based on the extremely detailed study of photocurrent multiplication measurements using a large number of wafers and GaAs *p-i-n* diodes. The measurements covered a very wide electrical field range (from 2×10^5 to 6×10^5 V/cm) with excellent reproducibility. To evaluate $E(x)$, Poisson's equation was solved neglecting the free hole contribution in the space-charge region, which is not important at the I_E values considered.

It can be seen from Fig. 6 that when the avalanche multiplication factor is calculated as a function of the local electric field, a large overestimation of the experimental data occurs, especially at low bias voltages. This observation means that the conventional impact ionization models, based on local electric field, cannot be used for the calculation of avalanche multiplication in *p-n-p* HBTs. We attribute the phenomenon to the fact that there is a strong dead space effect in *p-n-p* AlGaAs/GaInAs HBTs. This can be understandable. For devices having low carrier concentration and wide active regions, such as the photomultiplication diode and traditional Si bipolar transistors, the dead space constitutes a small fraction of the total depletion region and its effects are negligible. However, for advanced HBT devices with narrow depletion region and heavier doping, the dead space can be very significant. In fact such a strong dead space effect of injected electron has also been found in *n-p-n* AlGaAs/GaAs HBTs.[4,6] The dead space concept will be confirmed through the following theoretical models.

D. Theoretical modeling of the dead space effect

In order to confirm the dead space effect, a simple theoretical model has been developed, which is similar to that proposed by Filteroft *et al.*[7] We assume that a hole injected into the depletion region must travel a finite distance x_{th} before causing ionization. In this dead space, the probability of ionization by the injected carrier is assumed to be zero, and x_{th} is defined by[14]

$$\varepsilon_{\text{th}} = \int_0^{x_{\text{th}}} E(x)dx, \quad (6)$$

where ε_{th} is the threshold energy for ionization initiated by hole and $E(x)$ is the electric field profile in the space-charge region of the collector. Solving the integral in Eq. (6) yields an expression for x_{th} given by[7]

$$x_{\text{th}} = \frac{E_m \sqrt{E_m^2 - 2\varepsilon_{\text{th}}\dfrac{dE}{dx}}}{\dfrac{dE}{dx}}, \quad (7)$$

where E_m is the maximum value of electric field occurring at the n^+p junction. E_m and dE/dx can be found by solving Poission's equation.

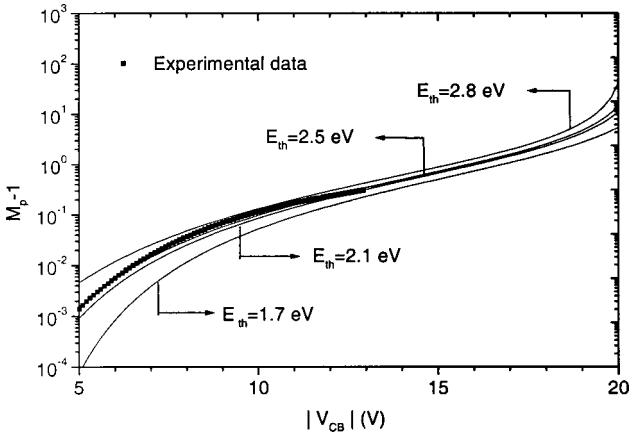

FIG. 7. Calculated multiplication factors as a function of applied voltage for different values of threshold energy.

In the dead space, α_p is zero for $0<x<x_{\text{th}}$ and only electrons entering from the collector region where $x>x_{\text{th}}$ contribute to impact ionization. We assume that electrons coming from outside the dead space, which cause impact ionization within the dead space, do not cause secondary ionization. Under these conditions, the electron current that can generate electron–hole pairs by impact ionization in the dead space may be assumed to be constant throughout the dead space. We also assume that the dead space effect for electrons generated near the subcollector is negligible. The effect of dead space on M_p may then be modeled by[15]

$$1-\frac{1}{M_p} = \left[1+\int_0^{x_{\text{th}}} \alpha_n(x)dx\right]\cdot\int_{x_{\text{th}}}^{W_C} \alpha_p(x) \times \exp\left\{-\int_{x_{\text{th}}}^{x}[\alpha_p(x')-\alpha_n(x')]dx'\right\}dx, \quad (8)$$

where $\alpha_n(x)$ and $\alpha_p(x)$ are given by Eqs. (4) and (5), respectively, and W_C is the width of collector space charge region. Capacitance–voltage measurements demonstrate that depletion region width is in excellent agreement with the collector width. The built in voltage was calculated to be 1.365 V for our device. Equation (8) was then solved using a numerical integral to find values of M_p-1 for the dead space corrected local model.

Figure 7 shows the theoretical results of avalanche multiplication factors for different values of threshold energy. It can be seen that, when threshold energy of 1.7, 2.1, and 2.8 eV is assumed, respectively, the dead space corrected model can not produce multiplication data to agree with the experimental results. When a threshold energy of 2.5 eV is assumed, the dead space corrected model produces multiplication data in excellent agreement with the experimental results.

Figure 8 shows the curve of dead space width x_{th} versus bias V_{BC}, which is calculated by the ensuing theoretical model. It demonstrates that the dead space constitutes a large fraction of the total depletion region, especially at low bias. For example, when the bias is 2, 4, and 6 V, the corresponding proportion of the dead space to total depletion region width is 55%, 35%, and 27%, respectively.

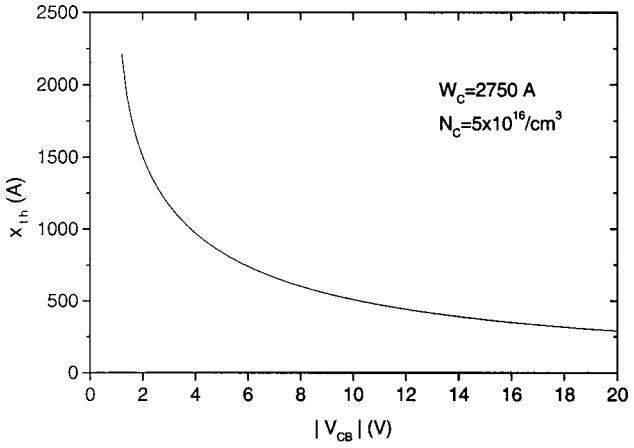

FIG. 8. Dead space width x_{th} as a function of the collector–base bias V_{BC}.

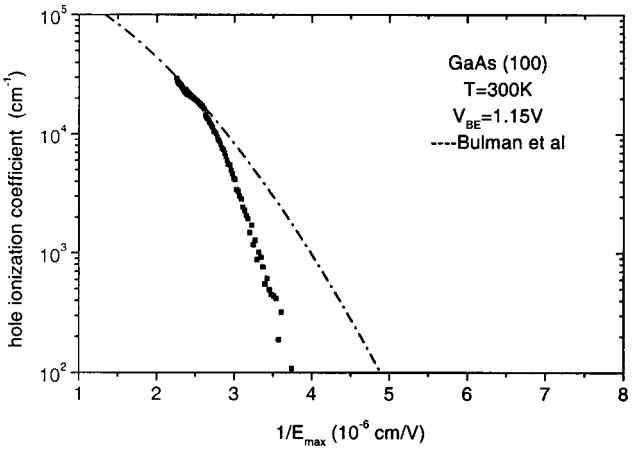

FIG. 9. Hole ionization coefficient in GaAs vs inverse electric field as obtained from collector multiplication factor measurement. Dashed line shows the results based on Ref. 14.

E. Hole-initiated impact ionization coefficient

In order to illustrate the effect of dead space on the impact ionization coefficient, the conventional deduction of α_p from M_p for the punchthrough condition was carried out in which α_p is assumed to depend only on the electric field. In the case of an abrupt n^+p junction at punchthrough, the hole ionization coefficient can be obtained by[16]

$$\alpha_p = \frac{E_m - E_d}{M_n M_p} \cdot \frac{dM_p}{dV_{\text{CB}}}, \tag{9}$$

where E_m and E_d are the maximum electric field at the n^+p junction and the electric field at the edge of the n region, respectively. Since our measurements only yield a multiplication factor for pure hole injection only, we approximate the electron multiplication as equal to hole multiplication, in order to deduce α_p. This approximation is justified at low electric fields where both electron and hole multiplication factor are very close to unity, and at higher electric fields where ionization coefficients for electrons and holes converge. Figure 9 shows hole ionization coefficient calculated from the multiplication factor measurement. The data of Bulman *et al.*calculated from expression (5) is also shown in Fig. 9. It can be seen that the α_p values agree with the data of Bulman *et al.* at high electric field, but fall significantly below bulk values at low electric fields. The lower the bias, the larger the departure. It demonstrates again that the conventional impact ionization models, based on local electric field, substantially overestimate the avalanche multiplication factor and hole ionization coefficient in p-n-p HBTs where significant dead space effects occur in the base–collector space-charge region.

It should be pointed out that, since the electric field varies fast in the collector, the holes might never reach their steady-state distribution. Therefore, using the concept of the electric dependent ionization coefficient outside the dead space in this article may give rise to certain inaccuracy in the calculation of the impact ionization rate as well as the estimation of the dead space width. The only accurate method to calculate the ionization rate is by Monte Carlo simulations[17,18] which take the energy distribution of holes in the collector into account. However, the approximation of this work is still effective. This has been confirmed by the excellent agreement between experimental results and the theoretical model of the dead space effect.

IV. CONCLUSION

In conclusion, measurements of the hole avalanche multiplication characteristics and ionization coefficient in AlGaAs/InGaAs p-n-p HBTs were performed and the results show that there is a strong dead space effect in p-n-p HBTs at low bias voltages. A local electric field model is not accurate for predicting the hole avalanche multiplication factor and impact ionization coefficient. Therefore, the nonlocal electric field effect will have to be taken into consideration to give a more accurate prediction of the avalanche multiplication effect in AlGaAs/GaAs p-n-p HBTs.

ACKNOWLEDGMENTS

This work is supported by a grant from the Research Grants Council of Hong Kong Special Administrative Region, China (Project No. HKU 7057/98E), and CRCG Grants (A/C Nos. 337/062/0047 and 10201982). The authors wish to thank Dr. Wang Hong for his suggestion and valuable discussions.

[1] B. Bayraktaroglu, Proc. IEEE **81**, 1762 (1993).
[2] W. Liu, E. Beam III, T. Kim, and A. Khatibzadeh, *Current Trends in Heterojunction Bipolar Transistors*, edited by M. F. Chang (World Scientific, Singapore, 1995).
[3] E. Zanoni, R. Malik, P. Pavan, J. Nagle, A. Paccagnells, and C. Canali, IEEE Electron Device Lett. **13**, 253 (1992).
[4] A. Di Carlo and P. Lugli, IEEE Electron Device Lett. **14**, 103 (1993).
[5] C. Canali, F. Capasso, R. Malik, A. Neviani, P. Pavan, C. Tedesco, and E. Zanoni, IEEE Electron Device Lett. **15**, 354 (1994).
[6] C. Canali, P. Pavan, A. Di Carlo, P. Lugli, R. Malik, M. Manfredi, L. Vendrame, and E. Zanoni, IEEE Trans. Electron Devices **43**, 1769 (1996).
[7] R. M. Fliteroft, J. P. R. David, P. A. Houston, and C. C. Button, IEEE Trans. Electron Devices **45**, 1207 (1998).
[8] D. Ritter, R. A. Hamm, A. Feygenson, and M. B. Panish, Appl. Phys. Lett. **60**, 3150 (1992).
[9] W. Liu, D. Hill, D. Costa, and J. S. Harris, IEEE Microwave Guid. Wave Lett. **2**, 331 (1992).
[10] D. B. Slater, Jr., P. M. Enquist, J. A. Hutchby, A. S. Morris, and R. J. Trew, IEEE Electron Device Lett. **15**, 91 (1994).

[11] W. Liu and J. S. Harris, IEEE Trans. Electron Devices **39**, 2726 (1992).
[12] N. Shamir and D. Ritter, IEEE Trans. Electron Devices **47**, 488 (2000).
[13] S. M. Sze, *Physics of Semiconductor Devices* (Wiley, New York, 1981).
[14] G. E. Bulman, V. M. Robbins, and G. E. Stillman, IEEE Trans. Electron Devices **32**, 2454 (1985).
[15] M. H. Woods, W. C. Johnson, and M. A. Lampert, Solid-State Electron. **16**, 381 (1973).
[16] G. E. Stillman and C. M. Wolfe, in *Semiconductors and Semimetals*, edited by R. K. Willardson and A. C. Beer (Academic, New York, 1977), Vol 12.
[17] J. Bude and K. Hess, J. Appl. Phys. **72**, 3554 (1992).
[18] M. V. Fischetti and S. E. Laux, Phys. Rev. B **38**, 9721 (1988).